JCTC Journal of Chemical Theory and Computation
Article
pubs.acs.org/JCTC

A meta-GGA Made Free of the Order of Limits Anomaly

Adrienn Ruzsinszky,[†] Jianwei Sun,[†] Bing Xiao,[†] and Gábor I. Csonka*[,†,‡]

[†]Department of Physics and Quantum Theory Group, Tulane University, New Orleans, Louisiana 70118, United States
[‡]Department of Inorganic and Analytical Chemistry, Budapest University of Technology and Economics, H-1521 Budapest, Hungary

Supporting Information

ABSTRACT: We have improved the revised Tao−Perdew−Staroverov−Scuseria (revTPSS) meta-generalized gradient approximation (GGA) in order to remove the order of limits anomaly in its exchange energy. The revTPSS meta-GGA recovers the second-order gradient expansion for a wide range of densities and therefore provides excellent atomization energies and lattice constants. For other properties of materials, however, even the revTPSS does not give the desired accuracy. The revTPSS does not perform as well as expected for the energy differences between different geometries for the same molecular formula and for the related nonbarrier height chemical reaction energies. The same order of limits problem might lead to inaccurate energy differences between different crystal structures and to inaccurate cohesive energies of insulating solids. Here we show a possible way to remove the order of limits anomaly with a weighted difference of the revTPSS exchange between the slowly varying and iso-orbitals (one- or two-electron) limits. We show that the new regularized (regTPSS) gives atomization energies comparable to revTPSS and preserves the accurate lattice constants as well. For other properties, the regTPSS gives at least the same performance as the revTPSS or TPSS meta-GGAs.

1. INTRODUCTION

The ascent of the ladder of nonempirical density functionals[1] generally results in better performance, although for several properties of bulk solids the second rung, the Perdew−Burke−Ernzerhof generalized gradient approximation (PBE GGA),[2,3] can be less accurate than local spin density approximation (LSDA). Predicting lattice constants more accurately than LSDA remained a challenge for a long time, even for state-of-the-art meta-GGA's. The nonempirical Tao−Perdew−Staroverov−Scuseria (TPSS) meta-GGA[4] only achieves a moderate improvement upon PBE GGA. Recently, we have used the PBEsol idea[5] to develop a revised TPSS or revTPSS[6] meta-GGA for atoms, molecules, solids, and surfaces. The basic idea of the PBEsol density functionals is to restore the second-order gradient expansion for exchange over a wide range of slowly or moderately varying densities.[5] The revTPSS meta-GGA preserves all the correct constraints of TPSS and keeps its good surface and atomization energies but yields lattice constants as good as those of the GGA's designed for solids. The revTPSS was designed to be a "workhorse density functional" for atoms, molecules, and solids.

Meta-GGA's are computationally not much more expensive than GGA's. It is expected that LSD and GGA users in condensed matter physics and quantum chemistry will switch to the meta-GGA, which can accurately describe both solids and molecules, at little extra cost.

All nonempirical meta-GGA functionals discussed here can be written in the form:[6]

$$E_{xc}[n_\uparrow, n_\downarrow] = \int d^3r n\varepsilon_{xc}(n_\uparrow, n_\downarrow, \nabla n_\uparrow, \nabla n_\downarrow, \tau_\uparrow, \tau_\downarrow) \quad (1)$$

where $n = n_\uparrow + n_\downarrow$ and τ_σ is the Kohn−Sham kinetic energy density of σ-spin electrons defined by

$$\tau_\sigma(r) = \frac{1}{2}\sum_i |\nabla \varphi_{i\sigma}(r)|^2 \quad (2)$$

where $\varphi_{i\sigma}$ are the occupied Kohn−Sham orbitals.

The meta-GGA exchange energy keeps $\varepsilon_x^{unif}(n) = -3\cdot(3\pi^2 n)^{1/3}/4\pi$, the exchange energy per electron for the uniform electron gas of density n, and adds the inhomogeneity parameters beyond the uniform electron gas by the enhancement factor:

$$E_x^{mGGA}[n] = \int d^3r n\varepsilon_x^{unif}(n)F_x^{mGGA}(p, z) \quad (3)$$

Here $p = s^2 = |\nabla n|^2/[4(3\pi^2)^{2/3}n^{8/3}]$ is the square of the dimensionless density gradient s, and

$$z = \frac{\tau_w}{\tau} \quad (4)$$

is an inhomogeneity parameter that arises beyond GGA. Regions of one- or two-electron density may be recognized by the condition $\tau = \tau_w$, where $\tau_w = |\nabla n|^2/8n$ is the Weizsäcker kinetic energy density. The parameter z falls in the range $0 \le z \le 1$; $z = 1$ for one- and two-electron densities, while $z = 5p/3 + O(\nabla^4) \to 0$ for slowly varying densities, for which the kinetic energy density has a second-order gradient expansion.[7] With these two limits of $z = 0$ or 1, the revTPSS satisfies two paradigms, the slowly varying limit relevant to condensed matter physics and the iso-orbital (one- or two-electron) limit relevant to quantum chemistry. In our recent meta-GGA development, the F_x is reduced for $z = 0$ and is kept at the TPSS limit at large s or for $z = 0$. With these constraints, we preserve the good lattice constants and surface properties and

Received: March 31, 2012
Published: May 11, 2012

 © 2012 American Chemical Society

the accurate atomization energies and enthalpies of formation at the same time.

Unlike in the exchange part, we do not in any case need to restore the correct gradient coefficient for correlation. For real densities the second-order gradient expansion for the correlation energy is never even close to being valid. The TPSS uses a constant correlation gradient coefficient, β, derived by Ma and Brueckner[8] in the high-density limit. Hu and Langreth[9] have derived the density dependence of β beyond the random phase approximation. We have fitted the β for revTPSS[6] roughly by

$$\beta(r_s) = 0.066725\frac{1 + 0.1r_s}{1 + 0.1778r_s} \tag{5}$$

where $n = 3/(4\pi r_s^3)$.

2. THE ORDER OF LIMITS PROBLEM

The general form of F_x has the fourth-order gradient expansion of the density:[10]

$$F_x = 1 + \left(\frac{10}{81}\right)p + \left(\frac{146}{2025}\right)q^2 - \left(\frac{73}{405}\right)pq + Dp^2 + O(\nabla^6) \tag{6}$$

where

$$q = \frac{\nabla^2 n}{(2k_F)^2 n} \tag{7}$$

For a slowly varying density we can find q from

$$\tilde{q}_b = \frac{9}{20}\frac{(\alpha - 1)}{[1 + b\alpha(\alpha - 1)]^{1/2}} + \frac{2}{3}p \tag{8}$$

with $b = 0.40$; $\tilde{q}_b$ is designed to remove the divergence of the exchange potential at the nucleus and to return the reduced Laplacian. The reduced Laplacian is also a measure of the inhomogeneity in the original fourth-order gradient expansion of ref 11.

In the general expression of eq 8, the ingredient α is

$$\alpha = \frac{5p}{3}\left[\frac{1}{z} - 1\right] \tag{9}$$

while z can be expressed by means of α:

$$z = \frac{1}{1 + \frac{3\alpha}{5p}} \tag{10}$$

In TPSS and revTPSS, F_x is constructed using both α and z, and then eq 10 is used to eliminate the z dependence. But in this equation, z has an unintended and unphysical order of limits anomaly:

$$\lim_{p\to 0}\lim_{\alpha\to 0} z = 1, \qquad \lim_{\alpha\to 0}\lim_{p\to 0} z = 0 \tag{11}$$

The different approach to zero in both α and p could lead to different limits of z and therefore different F_x values ($\lim_{p\to 0}F_x(p, \alpha = 0) = 1.1470$ and $\lim_{\alpha\to 0}F_x(p = 0, \alpha) = 1.0143$), as can be seen in Figure 1. There is a similar problem in TPSS and revTPSS correlation. This problem was noticed in early molecular tests of TPSS,[11] where it seemed to be harmless. But it may not be harmless in systems where important single-bond regions have both small α and small p (around the bond critical points). Single bonds are frequent in covalent molecules and in insulating solids where each atom in a solid has a large number of nearest neighbors with which it can form bonds. This is why the order of limits anomaly is particularly relevant for these solids and covalent molecules. The order of limits anomaly does not arise when α is zero but p is large, i.e., in an atom or in lone molecular orbitals filled by one or two electrons.

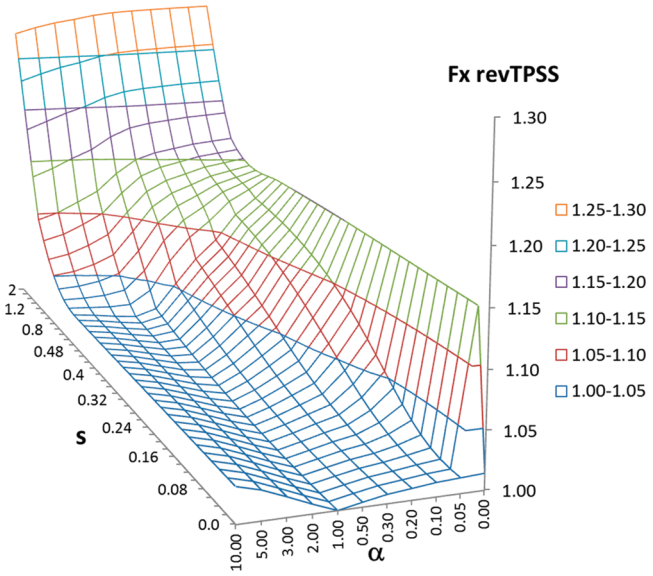

Figure 1. The two-dimensional surface of the revTPSS exchange-only enhancement function, $F_x(s, \alpha)$, where s is the reduced exchange gradient and α is defined by eq 9. The transparent surface shows the function values in the nonequidistant grid points connected by grid lines. The contour lines are shown for $F_x(s,\alpha = 1.05, 1.10, 1.15$, etc.). All parameters are in au. Notice the coordinates.

The order of limits problem can be the source of several failures in describing materials properties. The revTPSS did not perform as well as expected for the energy differences between different geometries for the same molecular formula and for the related nonbarrier height chemical reaction energies. This problem seems similar to the problem of the energy differences between different crystal structures and the problem of the cohesive energies of the insulating solids.

3. REMOVING THE ORDER OF LIMITS PROBLEM

We found that the order of limits problem can be removed by a weighted difference of the revTPSS F_x at $\alpha = 0$ and ordinary α values:

$$F_{x\mathrm{regTPSS}}(s, \alpha) = F_{x\mathrm{regTPSS}}(s, \alpha) + f(\alpha)\exp(-cs^2)[F_{x\mathrm{regTPSS}}(s, \alpha = 0) - F_{x\mathrm{regTPSS}}(s, \alpha)] \tag{12}$$

where $f(\alpha) = (1 - \alpha)^3/(1 + (d\alpha)^2)^{1.5}$, $c = 3$, and $d = 1.475$. In eq 12 we subtract a term that carries the entire order of limits problem and little else. The factor $f(\alpha)$ is designed to preserve the exact fourth-order gradient expansion of the revTPSS. In this new F_x, the natural ingredient is α instead of z. The values of c and d parameters were set by two criteria: Figure 1 shows that the order of limits anomaly does not arise for $s > 1$, so we set the value of $f(\alpha)\exp(-cs^2) = 0.001$ for $s = 1$. The second criterion was chosen to obtain flat $F_{x\mathrm{regTPSS}}$ surface for $s < 1$ and $\alpha > 1$ values.

dx.doi.org/10.1021/ct300269u | J. Chem. Theory Comput. 2012, 8, 2078−2087

For $\alpha = 0$, we recover F_x of revTPSS for the iso-orbital region. For $\alpha \approx 1$ the form of F_x becomes the F_x of revTPSS. The form above regularizes the revTPSS exchange close to those regions where both α and the gradient are small. The single bond in H_2, which has $\alpha = 0$, will then not be affected by the change from revTPSS to regTPSS, but other single bonds, including bonds to H, should be strengthened.

Comparison of Figures 1 and 2 shows that in the region of small α and s the difference between the regTPSS and the revTPSS is especially large. This is the region where z suddenly switches from 1 to 0, causing a sudden unphysical switch in $F_x(s, \alpha)$ at the same time (cf. Figure 1). The integration in eq 3 might smooth these wild oscillations out, but numerical problems might arise in the grid points, and the derivation results might be uncertain around such points. The contributions that arise from the difference $\exp(-cs^2)$-$[F_{x\mathrm{revTPSS}}(s, \alpha = 0) - F_{x\mathrm{revTPSS}}(s, \alpha)]$ smooth the change of F_x between $\alpha = 1$ and $\alpha = 0$, removing the order of limits anomaly and the sudden jumps in the F_x value for ($s < 0.2$, $\alpha < 0.05$) that are clearly visible in Figure 1. The Gaussian damping factor, $\exp(-cs^2)$, makes the correction disappear for the large gradient values. In this region the order of limits problem does not occur, and we keep the well performing revTPSS exchange (cf. Figures 1 and 2). Notice the considerable differences between the revTPSS and regTPSS $F_x(s, \alpha)$ surfaces for $\alpha > 1$ and $s < 0.4$. The revTPSS similar to TPSS shows a minimum at $\alpha = 1$ as a consequence of the gradient expansion. The regTPSS shows a very shallow minimum at $\alpha = 1$, and the surface is practically flat for $10 > \alpha > 1$ (cf. Figure 2); see also the related discussion of the calculated lattice constants in ref 12. This paper explores the large α behavior that is important in intershell regions while preserving revTPSS for α equal to 0 and 1. It is possible to construct an enhancement factor consisting of α or z ingredients but not both. Such a meta-GGA would be automatically free of the unphysical order of limits anomaly.

Test calculations show that the new regTPSS exchange functional does not work well with the revTPSS correlation (cf. Table 1). This is not surprising as revTPSS correlation was constructed to work with an exchange functional that includes the order of limits anomaly. Thus we applied a modified PBE correlation functional. In this refined PBE functional, the β coefficient value is not the fixed high-density limit (as suggested in the original PBE paper), but it takes a density-dependent form as shown in eq 5 (we call this regTPSS correlation functional). The new regTPSS exchange and correlation works quite well together as shown in Tables 1−3. The price we pay for using this regTPSS correlation functional is the loss of the one-electron self-correlation freedom of the revTPSS correlation functional. The one-electron self-correlation error artificially stabilizes the H atom by 3.95 kcal/mol. This stabilization, however, does not result in a serious underbinding error for the atomization energies of hydrogen-containing molecules. For the H_2 molecule, the 5.0 kcal/mol overbinding error of the revTPSS is changed to 2.8 kcal/mol underbinding error of the regTPSS. For the octane molecule (C_8H_{18}), the revTPSS yields a small 1.6 kcal/mol overbinding error, while the regTPSS yields 11.5 kcal/mol underbinding error. This shows that the one-electron self-correlation freedom might help to obtain improved atomization energies for the compounds that contain many H atoms. But notice that molecular reaction energies are not influenced by the atomic energy errors.

Figure 3 shows the revTPSS and regTPSS exchange−correlation enhancement $F_{xc}(s, \alpha, r_s)$ curves. As the regularization of the revTPSS functional does not change the exchange enhancement factor for $\alpha = 0$ and 1, comparison of the relevant revTPSS and regTPSS curves shows clearly the effects of the modified correlation functional (cf. Figure 3 and Figure S1, Supporting Information). Notice the large difference between the $F_{xc}(s, \alpha, r_s)$ for $\alpha = 0$ and $r_s = 1000$ in the Figure 3. For larger electron densities the differences between the two curves gradually decrease (cf. $r_s = 1$ curves), and for very large electron densities (e.g., $r_s = 0.001$), the two curves agree with each other as shown in Figure 3. The lower part of the Figure 3 shows the dramatic difference between the revTPSS and regTPSS $F_{xc}(s, \alpha, r_s)$ for small $\alpha = 0.02$ and $s < 0.5$. The steep decrease of the revTPSS $F_{xc}(s, \alpha, r_s)$ curves is very different from the almost constant value of the regTPSS curves in this range of parameters. This is the main effect of the regularization. Figure S1, Supporting Information, shows similar comparisons of revTPSS and regTPSS $F_{xc}(s, \alpha, r_s)$ for $\alpha = 0.1$, 0.25, 0.5, 1, 2, 4, and 1000. For small $\alpha = 0.1$, 0.25

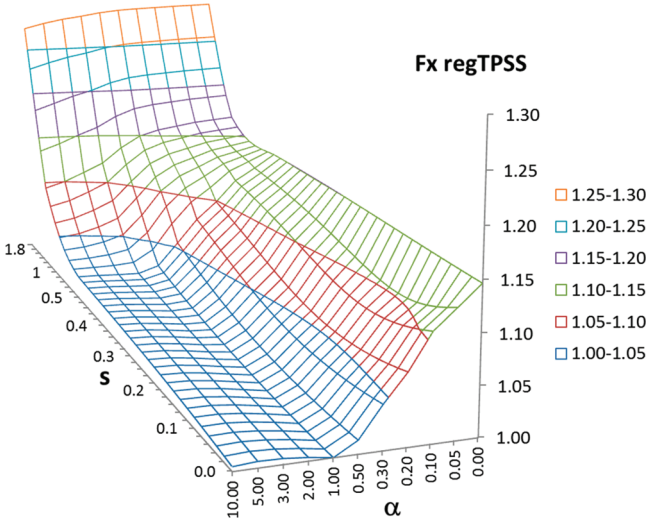

Figure 2. The two-dimensional surface of the regTPSS exchange-only enhancement function, $F_x(s, \alpha)$, where s is the reduced exchange gradient and α is defined by eq 9. The transparent surface shows the function values in the nonequidistant grid points connected by grid lines. The contour lines are shown for $F_x(s, \alpha = 1.05, 1.10, 1.15$, etc.). All parameters are in au. Notice the coordinates.

Table 1. Atomization Energies of the AE6 Molecules, in kcal/mol, Calculated Self-Consistently from Gaussian Using the Aug-cc-pV5Z Basis Set and Standard Geometries[a]

molecule	TPSS	revTPSS	regTPSS	regTPSS−TPSS	expt.
SiH_4	333.7	338.2	327.6	339.7	322.4
SiO	186.7	185.7	184.1	183.1	192.1
S_2	108.7	109.1	107.9	107.6	101.7
C_3H_4	707.5	704.1	701.9	712.3	704.8
$C_2H_2O_2$	636.0	632.8	633.3	635.9	633.4
C_4H_8	1155.5	1153.4	1149.1	1171.8	1149.0
ME	4.1	3.3	0.1	7.8	
MAE	5.9	5.9	3.7	10.8	
MRE (%)	1.5	1.5	0.5	1.7	
MARE (%)	2.4	2.7	2.1	3.2	

[a]As in ref 11.

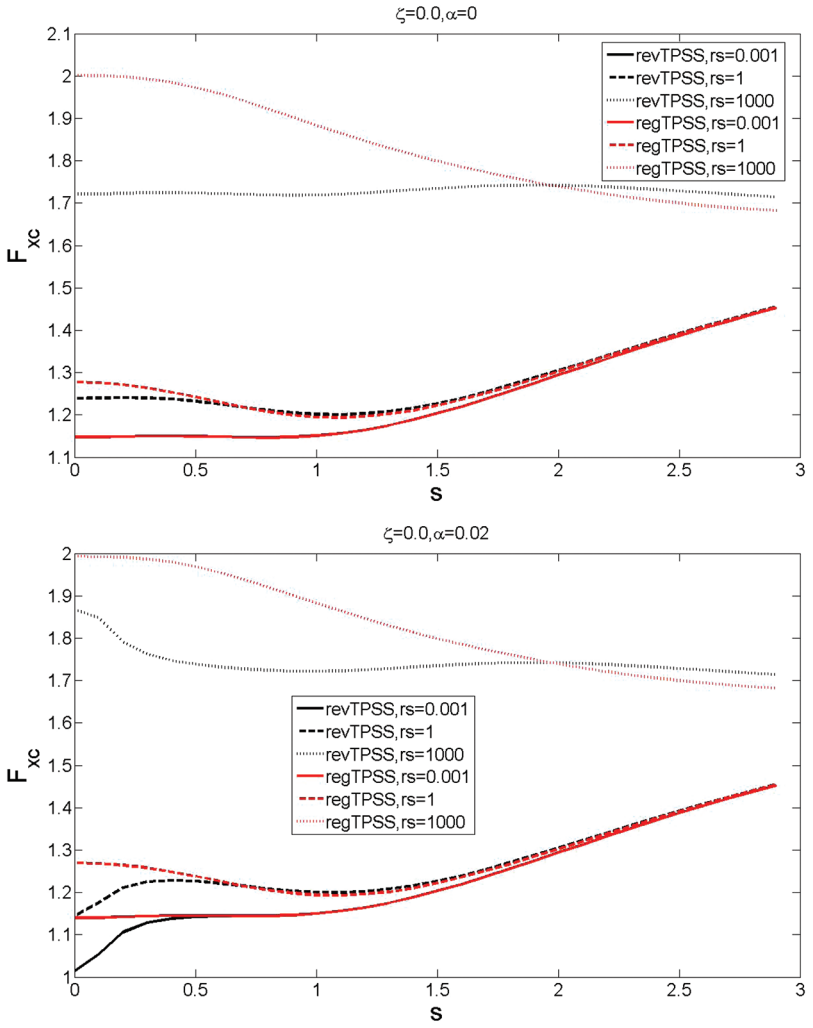

Figure 3. Comparison of the values of the revTPSS and regTPSS exchange−correlation enhancement functions, F_{xc}, as functions of the reduced exchange gradient, s, α of eq 9, and Wigner−Seitz radius, r_s for the spin unpolarized case ($\zeta = 0$). All parameters are in au.

values, a considerable difference can be observed between the revTPSS and regTPSS curves for $s < 0.5$ and $r_s < 1$. This difference almost disappears for $\alpha = 0.5$, 1, and 2. For $\alpha = 4$ and 1000, the regTPSS $F_{xc}(s, \alpha, r_s)$ values are smaller than the corresponding revTPSS values, in agreement with flat surface of regTPSS $F_x(s, \alpha)$ for $\alpha > 1$, as shown in Figure 2.

4. RESULTS

To test our new regTPSS functional, we calculated atomization energies, enthalpies of formation, hydrogen bonds, lattice constants, cohesive energies, bulk moduli, structural phase transitions, and adsorption energies for the adsorption of CO on a metal surface. For the lattice constants, the bulk moduli, and cohesive energies, for comparison we show results obtained with other semilocal density functionals, like LSDA, PBE, PBEsol, TPSS, and revTPSS, too. These test sets serve for comparison of the performance of the new regTPSS functional with the performance of the previous revTPSS functional, and thus they are not as representative as the considerably larger composed test sets proposed by Grimme. However, we also test the performance for solid-state properties, and in this sense, we go beyond those molecular test sets and show a more balanced picture of the performance.

The regTPSS was implemented self-consistently in the VASP[13] plane-wave solid-state program, while for the molecular calculations we used the Gaussian program package[14] with a non-self-consistent implementation of the regTPSS density functional.

First we tested our new form on the small but somewhat representative[15] AE6 test set[16] composed of atomization energies of six molecules: SiH_4, SiO, S_2, C_3H_4, $C_2H_2O_2$, and C_4H_8. The results calculated with aug-cc-pV5Z basis set are shown in Table 1. We have also performed regTPSS calculations with the VASP code as well (not shown in Table 1) and obtained mean absolute error (MAE) = 4.3 kcal/mol that agrees reasonably well with the 3.7 kcal/mol value shown in the Table 1 despite the very different approaches used by VASP and Gaussian programs for calculation of the atomization energies. The regTPSS results are more accurate than the quite good revTPSS results for the AE6 data set. Moreover the mean error (ME) value of the regTPSS shows no overbinding for the atomization energies in contrast with the small but typical overbinding of TPSS. The smaller basis sets that underbind compensate efficiently the TPSS overbinding error.[17] Notice that the compensation of the overbinding error of a functional by an underbinding error of a basis set is not a reliable procedure, and unexpected failures might occur. The regTPSS

meta-GGA requires large, good-quality basis sets for good results. Our regTPSS/6-311+G(3df,2p) results (ME = 0.0 and MAE = 3.8 kcal/mol) show an excellent agreement with the results in Table 1. Thus this smaller basis set is practically converged and can be used for benchmarking the functional on larger test sets. As the exact exchange mixing compensates the overall overbinding of the parent functional,[15] the regTPSS hybrid will not show improved atomization energy results. The results in Table 1 also show the serious overbinding (7.8 kcal/mol) of the regTPSS exchange combined with the TPSS correlation functional. This functional requires larger exact exchange mixing (20−25%) than TPSS (10%) for improved thermochemistry results, but this is not investigated further in this paper.

Next we test the regTPSS for the enthalpies of formation of the 223 molecules in the G3/99 test set,[18] which is composed of the G2-1, G2-2 and G3-3 subgroups. The G1-1 and G1-2 mostly contain small molecules and radicals, while the G3-3 contains larger organic molecules and difficult inorganic radicals. This test set is considerably more representative than the small AE6 test set. It is time consuming so we had to use a less expensive 6-311+G(2df,2p) basis set instead of the very expensive aug-cc-pV5Z. The statistical results in Table 2 show the overall performance of the new regTPSS is slightly better than the performance of the TPSS but slightly worse than the performance of the revTPSS. The new regTPSS shows good performance for the small molecules (G2-1 and -2), but it performs poorer for the large organic molecules where revTPSS is clearly superior to TPSS.

Table 2. Comparison of Various Functional for the G3-99 and Various Subsets of the G3-99 Test Sets[a]

		TPSS	revTPSS	regTPSS
G3-99	ME	−5.07	−3.60	0.53
	MAE	5.70	4.81	5.43
	RMSE	6.77	6.53	7.14
	SD	4.49	5.45	7.14
	max	16.20	16.39	30.50
	min	−22.93	−25.71	−19.50
G2-1	ME	−3.61	−3.25	0.09
	MAE	4.47	4.80	4.51
	RMSE	5.71	6.59	5.31
	SD	4.47	5.79	5.36
	max	5.61	7.94	13.80
	min	−18.03	−24.59	−9.90
G2-2	ME	−6.03	−4.53	−0.15
	MAE	6.77	5.61	4.85
	RMSE	7.86	7.29	7.03
	SD	5.07	5.75	7.07
	max	16.20	16.39	30.50
	min	−22.93	−25.71	−18.50
G3-3	ME	−4.97	−2.71	1.68
	MAE	5.26	3.81	6.83
	RMSE	5.98	5.36	8.36
	SD	3.36	4.66	8.24
	max	7.73	4.74	20.70
	min	−12.75	−18.21	−19.50
G3-org	ME	−5.08	−1.58	2.14
	MAE	5.11	2.70	6.43
	RMSE	5.71	3.57	7.77
	SD	2.63	3.24	7.53
	max	0.51	4.74	16.60
	min	−12.57	−11.85	−19.10

[a]All statistical errors are in kcal/mol. Calculations with 6-311+G(2df,2p) basis sets.

For general utility it is advantageous if a functional performs well not only for molecules but for solids too. Table 3 shows the performance of the regTPSS compared to several earlier functionals (LDA, PBE, PBEsol, revTPSS). The correct prediction of lattice constants is of key interest for solid-state applications and materials design. We use experimental lattice constants corrected for thermal effects and zero-point anharmonic expansion (ZPAE as shown in the table) as reference.[19] The statistics in the Table 3 shows that the new regTPSS performs best. We have also calculated the statistics compared to the zero-point phonon corrected experimental results[20] (not shown here), but the statistics did not change. In Figure 4 we ordered the solids according to the LDA error. The LDA gives systematically too small lattice constants, but it performs very well for Ge, SiC, Si, MgO and diamond (C). Figure 4 shows that PBE occasionally overcorrects this LDA error, showing very large error for Ge, but it gives a reasonably good result for diamonds. On average PBE gives a too large positive correction to LDA lattice constants and performs well where the LDA lattice constants are too short (e.g., for Na, Ca, Sr, Ba; cf. Figure 4). For Ca, Sr, and Ba, the PBEsol correction to the LDA lattice constant is too small, and the PBEsol shows the largest errors for these solids. Here the regTPSS functional performs quite well. The new regTPSS compensates much better the LDA errors than the PBE, even better than the already good PBEsol, and performs best among the functionals studied here followed by the revTPSS functional.

The results in Table 4 show that for bulk moduli, PBEsol performs best followed by the regTPSS functional. The latter is clearly superior over the TPSS and revTPSS functionals. The experimental ZPAE-corrected reference values are taken from refs 19 and 21.

For cohesive energies of the selected solids in the Table 5 PBE give the best MAE and MARE (%) values. While regTPSS and revTPSS compensate the large overbinding LDA errors and do not show the small underbinding error of the PBE, their overall performance is somewhat worse. In this respect the regTPSS functional does not reach the performance of the HSEsol[21] functional. The reference experimental cohesive energies are taken from Table 5 of ref 21, except for Ca, Sr, and Ba. The experimental values for those solids are taken from ref 22, and zero-point vibration energy (ZPVE) corrections are taken from Table 5 of ref 23.

Next we analyze the performance of several density functionals shown in Table 6 for the phase transition energies and pressures of solid Si and SiO_2 crystals. We have calculated the total energies and energy differences of Si in metallic β-Sn and insulating diamond phases and SiO_2 in the α-quartz and stishovite phases at the calculated equilibrium volumes (T = 0 K, P = 0 Pa) by VASP plane-wave pseudopotential program (PAW, Si_d_GW, O_GW pseudopotentials, kinetic energy cutoff 500 eV, Monkhorst−Pack,[24] 16 × 16 × 16 k mesh).

Under pressure, Si displays 11 phases with a transition from semiconductor to metal.[25] At standard pressure, Si occurs in the diamond structure. At a pressure of 11.3−12.6 GPa, Si transforms to the metallic β-Sn structure (increase in the coordination number from 4 to 6 and decrease in the volume by 21%). Earlier DMC[26] and HSE06[27] calculations found that the energy differences between diamond and β-Sn Si are

Table 3. Lattice Constants (Å) Calculated with Various DFT Methods Compared to ZPAE Corrected Experimental Values[a]

solids	LDA	PBE	PBEsol	TPSS	revTPSS	regTPSS	expt. (ZPAE corrected)
Li	3.362	3.431	3.426	3.448	3.440	3.439	3.453
Na	4.051	4.198	4.170	4.239	4.215	4.219	4.214
Ca	5.332	5.518	5.448	5.522	5.504	5.513	5.553
Sr	5.791	6.027	5.916	6.028	6.007	5.999	6.045
Ba	4.770	5.030	4.894	5.009	4.986	4.975	4.995
Al	3.983	4.035	4.011	4.008	4.005	4.006	4.018
Cu	3.522	3.633	3.565	3.580	3.559	3.554	3.595
Rh	3.759	3.831	3.781	3.805	3.785	3.782	3.794
Pd	3.844	3.942	3.876	3.904	3.884	3.879	3.876
Ag	4.002	4.145	4.050	4.086	4.052	4.048	4.062
C	3.533	3.569	3.552	3.568	3.558	3.553	3.553
SiC	4.332	4.378	4.355	4.366	4.357	4.356	4.346
Si	5.405	5.468	5.432	5.453	5.439	5.431	5.421
Ge	5.631	5.768	5.680	5.729	5.682	5.689	5.644
GaAs	5.615	5.752	5.665	5.718	5.680	5.673	5.640
LiF	3.913	4.070	4.007	4.050	4.029	4.016	3.972
LiCl	4.968	5.151	5.063	5.121	5.109	5.087	5.070
NaF	4.506	4.705	4.632	4.710	4.680	4.664	4.582
NaCl	5.467	5.695	5.603	5.701	5.667	5.645	5.569
MgO	4.170	4.261	4.223	4.244	4.240	4.230	4.189
ME	−0.082	0.051	−0.012	0.035	0.014	0.008	
MAE	0.082	0.060	0.035	0.043	0.032	0.028	
MRE (%)	−1.73	1.10	−0.24	0.73	0.29	0.16	
MARE (%)	1.73	1.29	0.73	0.90	0.68	0.60	

[a]The corrected experimental values are taken from ref 19.

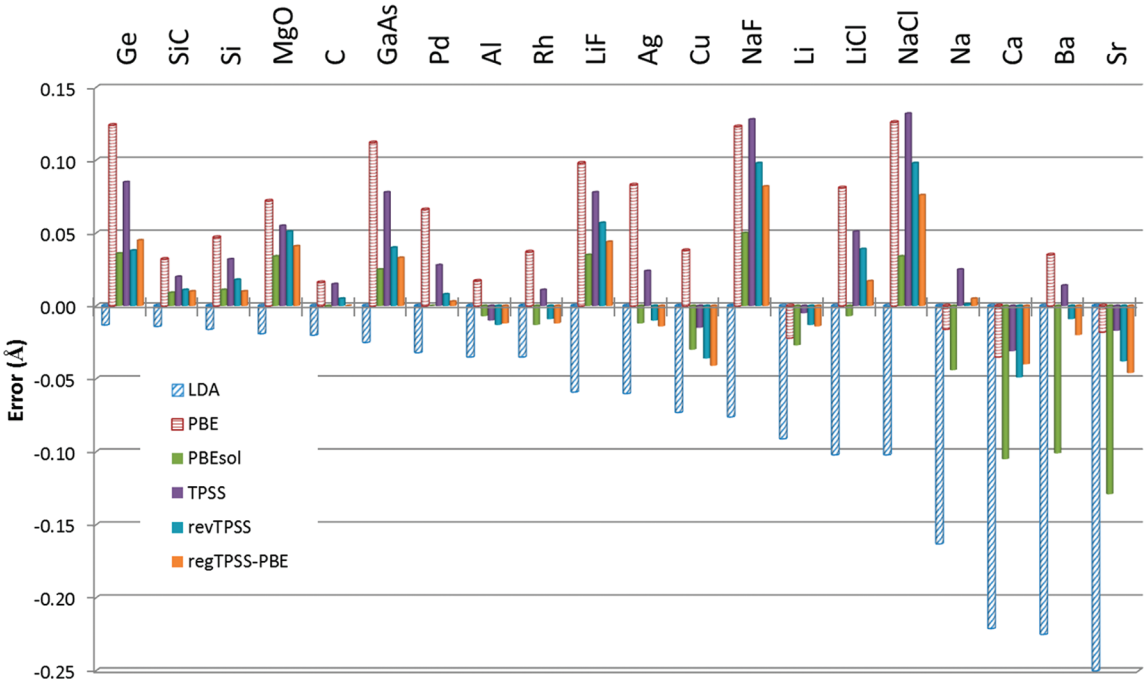

Figure 4. Comparison of the errors (calculated expt. in Å) of the lattice constants calculated with LDA, PBE, PBEsol, TPSS, revTPSS, and regTPSS functionals. The errors were calculated relative to the ZPAE corrected experimental values.

0.424(20) eV/atom (cf. Table 6) and 0.390 eV/atom, respectively (cf. ref 26). These values are supposed to be of good quality, and we use these as references. The regTPSS energy difference is 0.285 eV/atom, similar to PBE (0.290 eV/atom) and TPSS (0.265 eV/atom) results. This is a significant improvement compared to revTPSS and PBEsol results. The regTPSS, TPSS, and PBE functionals give considerably better phase transition pressures than LSDA, PBEsol, and revTPSS (cf. Table 6) if compared to the experimental value from ref 28. In Table 6 we present our theoretical values without any correction. Thus comparison of theoretical and experimental values needs some considerations. One of the difficulties arises

dx.doi.org/10.1021/ct300269u | J. Chem. Theory Comput. 2012, 8, 2078−2087

Table 4. Bulk Moduli (GPa) Calculated with Various DFT Methods Compared to Zero-Point Phonon Effects (ZPPE) Corrected Experimental Values[a]

solids	LDA	PBE	PBEsol	TPSS	revTPSS	regTPSS	expt. ZPAE
Li	15.1	13.8	13.7	13.3	13.4	13.4	13.9
Na	9.2	7.8	7.8	7.3	7.5	7.4	7.7
Ca	19.4	17.5	17.9	17.6	17.9	17.6	18.7
Sr	14.5	11.1	12.9	10.7	10.9	11.1	12.5
Ba	10.6	8.8	9.4	8.4	8.7	8.7	9.4
Al	83.7	77.3	81.9	85.6	85.7	84.7	82
Cu	187.4	138.0	166.0	162.4	173.8	175.8	145
Rh	315.6	256.4	295.0	281.9	296.1	298.9	272.1
Pd	226.3	169.4	205.2	195.4	209.7	210.7	198.1
Ag	138.5	90.9	118.9	110.0	120.5	121.7	110.8
C	465.8	433.2	450.2	430.3	439.5	450.7	454.7
SiC	229.5	212.8	221.9	217.2	221.5	224.6	229.1
Si	97.0	90.0	92.8	92.0	93.0	98.8	100.8
Ge	70.5	59.4	65.8	60.2	65.0	67.8	77.3
GaAs	75.1	60.5	69.9	64.8	66.8	69.1	76.7
LiF	86.7	66.9	72.2	66.2	68.9	70.05	76.3
LiCl	41.5	31.7	35.4	33.4	34.0	34.6	38.7
NaF	61.5	45.2	48.8	42.9	44.0	45.6	53.1
NaCl	31.2	23.6	26.0	22.4	24.1	24.3	27.6
MgO	172.1	149.5	157.6	155.0	155.5	158.4	169.8
ME	8.8	−10.5	−0.3	−4.9	−0.9	1.0	
MAE	10.1	10.5	6.2	7.9	8.7	7.4	
MRE (%)	9.3	−10.5	−1.9	−7.7	−4.3	−3.0	
MARE (%)	10.8	10.6	5.7	9.6	9.0	8.1	

[a]The corrected experimental values are taken from ref 21, except for Ca, Sr, and Ba. The corrected experimental values for those solids are taken from ref 19.

Table 5. Cohesive Energies (eV/atom) Calculated with Various DFT Methods Compared to ZPVE Corrected Experimental Values[a]

solids	LDA	PBE	PBEsol	TPSS	revTPSS	regTPSS	expt. ZPVE corr.
Li	1.81	1.61	1.68	1.63	1.64	1.52	1.66
Na	1.26	1.08	1.15	1.14	1.15	1.08	1.12
Ca	2.22	1.92	2.12	2.03	2.07	2.08	1.86
Sr	1.89	1.61	1.81	1.75	1.82	1.85	1.73
Ba	2.25	1.87	2.11	2.02	2.09	2.13	1.91
Al	4.04	3.44	3.82	3.48	3.57	3.53	3.43
Cu	4.54	3.47	4.03	3.79	4.12	4.11	3.52
Rh	7.56	5.69	6.64	5.78	6.16	5.99	5.78
Pd	5.02	3.71	4.44	3.98	4.38	4.34	3.94
Ag	3.64	2.52	3.08	2.73	3.03	3.02	2.98
C	9.01	7.71	8.28	7.25	7.31	7.46	7.55
SiC	7.21	6.40	6.88	6.19	6.25	6.33	6.48
Si	5.35	4.56	4.94	4.43	4.50	4.61	4.68
Ge	4.63	3.72	4.14	3.64	3.78	3.79	3.92
GaAs	4.69	3.15	3.56	3.12	3.26	3.27	3.34
LiF	4.14	4.32	4.47	4.22	4.23	4.13	4.46
LiCl	2.94	3.36	3.52	3.36	3.39	3.32	3.59
NaF	4.47	3.83	3.96	3.74	3.74	3.66	3.97
NaCl	3.50	3.10	3.22	3.10	3.14	3.08	3.34
MgO	6.61	4.97	5.30	4.94	4.93	4.95	5.20
ME	0.62	−0.12	0.23	−0.11	0.01	−0.01	
MAE	0.71	0.14	0.25	0.17	0.21	0.20	
MRE (%)	15.86	−3.68	5.97	−1.99	1.22	0.37	
MARE (%)	18.38	4.23	6.52	4.70	5.73	6.09	

[a]The corrected experimental values are taken from ref 21, except for Ca, Sr, and Ba, The experimental values for those solids are taken from ref 22 and 0.01−0.02 eV/atom ZPVE corrections are added according to Table 5 of ref 23.

Table 6. Calculated Phase Transition Energy Differences (ΔE_e) and Phase Transition Pressures (P_{tr}) of Si in the β-Sn and Diamond Phases and of SiO_2 in the α-Quartz and Stishovite Phases at the Equilibrium Volumes

		LSDA	PBEsol	PBE	TPSS	revTPSS	regTPSS	HSE06	DMC	expt.
Si phase transition	ΔE_e (eV/atom)	0.206	0.185	0.290	0.265	0.160	0.284	0.390[a]	0.424(20)[a]	
	P_{tr} (GPa)	5.8,[a] 7.0	4.8,[a] 6.1	8.4,[a] 9.7	8.6	5.0	9.3	12.4[a]	14.0 ± 1.0[a]	11.3−12.6[b]
SiO_2 phase transition	ΔE_e (eV/SiO_2)	−0.030	0.171	0.532	0.383	0.208	0.167	0.494	0.495(11)[c]	0.51−0.54[d]
	P_{tr} (GPa)	−0.4	2.1	6.4	3.3	2.1	1.9	5.6	6.3 ± 0.5[c]	7.5[e]

[a]From ref 26, the calculated values contain −1.3 GPa finite temperature and zero point energy corrections. [b]Ref 28. [c]Ref 32. [d]Refs 30 and 31. [e]Ref 31.

from the fact that the theoretical works usually report the coexistence pressure, while the diamond to β-Sn phase transition in silicon is irreversible in the experiment (different structural phases are found on decompression). Consequently the coexistence pressure cannot be bracketed experimentally by compression and decompression. The experimental results also contain temperature and zero-point energy effects. Another difficulty is that the calculation of the temperature and zero-point energy effects requires heavy computational efforts and might be inaccurate. Recent phonon calculations[29] give reduction in the transition pressure from zero-point motion of about 0.62 GPa and a further reduction of 0.34 GPa at 300 K. More than a 30% larger 1.3 GPa reduction was given in ref 26. With this latter correction, our values agree well with the values in ref 26. The uncertainties in the temperature and zero-point energy effects do not change our conclusion: The regTPSS introduces changes in the right direction.

For the SiO_2 α-quartz to stishovite phase transition, the regTPSS energy difference is quite poor (0.16 eV/SiO_2) and is significantly smaller than the experimental value in Table 6 (0.51−0.54 eV/SiO_2).[30,31] The DMC[32] and PBE phase transition pressures agree quite well (cf. Table 6, 6.3 ± 0.5 and 6.5 GPa, respectively). The HSE06 phase transition energy difference agrees particularly well with DMC results, but PBE results agree better with experiment. The very expensive thermal and zero-point energy corrections calculated by CASTEP[33] code yield that the transition pressure is increased by 0.55 GPa at 300 K. This correction yields good agreement between PBE and experimental results. LSDA has a sign error, and the small gradient enhancement coefficient, μ, used for exchange in PBEsol, revTPSS and regTPSS does not yield a sufficient improvement as shown in Table 6. Earlier studies of siloxane, the prototype molecule of Si−O−Si structure showed that the correct description of the potential energy surface of this structure is very challenging,[34−37] but DFT calculations can come close to CCSD(T)/cc-pVTZ results.[35] In a future study, we plan to analyze the source of the errors for the SiO_2 α-quartz to stishovite phase transition.

We have also tested the regTPSS on the famous CO/Pt(111) puzzle,[38,39] which states that the standard semilocal functionals put the CO molecule on the hollow fcc site of the Pt (111) surface rather than the experimentally observed top site. Table 7 shows the desorption energies of CO on the hollow fcc and top sites of the Pt (111) surface for regTPSS, revTPSS, PBE, PBEsol, and LDA. The literature overview and the computational details can be found in the ref 41. The desorption energies improve and the surface energies deteriorate by increasing the GGA exchange enhancement factor from PBEsol to PBE (because GGAs cannot handle differently the same reduced density gradient in different regions).[40,41] Large μ is required for good top desorption energy, but this results in a too small Pt surface energy (PBE).

Table 7. Desorption Energies (eV) of CO on Different Sites of the Pt (111) Surface[a]

	LDA	PBEsol	PBE	revTPSS	regTPSS	expt.[38]
E_{des_fcc}	2.66	2.27	1.82	1.72	1.71	
E_{des_top}	2.29	1.98	1.67	1.55	1.58	1.37 (0.13)
fcc top	0.37	0.29	0.15	0.17	0.12	

[a]E_{des_fcc} and E_{des_top} are the desorption energies for the hollow fcc and top sites, respectively. The last row shows $E_{des\_fcc} - E_{des\_top}$ with positive values indicating preference for the fcc site. The experimental value is given for the experimentally observed top site with the uncertainty in parentheses.

Decreasing the value of μ leads to poor top desorption energies but improves considerably the Pt surface energies (PBEsol). Notice that LDA gives the best surface energy and the largest positive error for the top desorption energy.[41] The revTPSS and regTPSS meta-GGAs improve the top desorption energies and the surface energies at the same time thus resolve this dilemma unsolvable at GGA level. But the incorrect energy difference between the top and hollow fcc sites is only slightly improved by regTPSS compared to revTPSS (cf. Table 7). Since regTPSS exchange-only regularizes the small s and small α region of revTPSS, which is not an important region for the CO molecule adsorbed on transition metal surfaces (where α values are around 1), regTPSS and revTPSS yield similar desorption energies. The new regTPSS meta-GGA yields quite good top desorption energy (1.58 eV) and shows the least incorrect CO adsorption site preference compared to LDA, PBEsol, PBE, and revTPSS functionals (cf. Table 7).

5. CONCLUSIONS

We have successfully removed the order of limits anomaly from the revised or revTPSS meta-GGA with a weighted difference of the revTPSS exchange between the slowly varying and iso-orbitals (one- or two-electron limits). The motivation for revTPSS was to keep good surface and atomization energies of TPSS and obtain lattice constants as good as those of the GGA designed for solids. The revTPSS recovers the second-order gradient expansion for a wide range of densities and therefore provides excellent lattice constants. However the revTPSS inherited the order of limits anomaly from TPSS, and this might lead to the inaccurate energy differences between different crystal structures and to the inaccurate cohesive energies of the insulating solids. Our new regularized regTPSS gives atomization energies comparable to revTPSS and preserves the accurate lattice constants as well. For other properties, the regTPSS gives at least the same performance as the revTPSS or TPSS meta-GGAs. Our main results in this paper are the following:

(1) The regTPSS results are more accurate than the quite good revTPSS results for the AE6 data set. The mean

absolute error is reduced from 5.9 to 3.7 kcal/mol. Moreover the ME value of the regTPSS shows no overbinding for the atomization energies in contrast with the small but typical overbinding of TPSS.

(2) The overall performance of the new regTPSS is slightly better for the G3/99 test set than the performance of the TPSS but slightly worse than the performance of the revTPSS. The new regTPSS shows good performance for the small molecules (G2-1 and -2), but it performs poorer for the large organic molecules where revTPSS is clearly superior to TPSS.

(3) For lattice constants of 20 solids, Li, Na, Ca, Sr, Ba, Al, Cu, Rh, Pd, Ag, C, SiC, Si, Ge, GaAs, LiF, LiCl, NaF, NaCl, and MgO, the new regTPSS performs best compared to LDA, PBE, PBEsol, TPSS, and revTPSS functionals.

(4) For bulk moduli of the same 20 solids, PBEsol performs best followed by the regTPSS functional. This latter is clearly superior over the TPSS and revTPSS functionals.

(5) For cohesive energies, the regTPSS and revTPSS correct the large overbinding LDA errors and do not show the small underbinding error of the PBE, but their overall performance is somewhat worse than the performance of the PBE or HSEsol.

(6) The regTPSS transition energy (0.284 eV/atom) and pressure (9.3 GPa) for the semiconducting diamond to metallic β-Sn phase transition in silicon is considerably better than those calculated by LSDA, PBEsol, and revTPSS (5.5 GPa phase transition pressure). The regTPSS phase transition pressure is better than the TPSS (8.7 GPa) and slightly worse than the PBE (9.7 GPa) result. The best phase transition pressure can be obtained by HSE06.

(7) For the SiO_2 α-quartz to stishovite phase transition, the regTPSS energy difference (0.16 eV/SiO2) is significantly smaller than the experimental value. The LSDA energy difference has a sign error, and the small gradient enhancement coefficient, μ, used for exchange in PBEsol, revTPSS, and regTPSS does not yield a sufficient improvement. PBE (large μ) shows an excellent agreement with experiment (better than HSE06), while TPSS performs poorly.

(8) For desorption energies of carbon monoxide, CO, from top and hollow fcc positions, of the Pt (111) surface, regTPSS and revTPSS yield similar desorption energies. The new regTPSS meta-GGA yields quite a good top desorption energy (1.58 eV) and shows the least incorrect CO adsorption site preference compared to LDA, PBEsol, PBE, and revTPSS functionals. The revTPSS and regTPSS meta-GGAs improve the top desorption energies, and the Pt surface energies at the same time thus resolve a dilemma unsolvable at GGA level.

These results show that it is possible to construct an order of limits anomaly-free TPSS-type functional, the regularized regTPSS functional, that performs as well as or better than the previous revTPSS functional. All these results show that the nonempirical meta-GGA can be improved further.

■ ASSOCIATED CONTENT

Supporting Information

Comparisons of revTPSS and regTPSS $F_{xc}(s, a, r_s)$ curves for a = 0.1, 0.25, 0.5, 1, 2, 4, and 1000 in s = 0−3 and r_s = 0.001−1000 range. This material is available free of charge via the Internet at http://pubs.acs.org.

■ AUTHOR INFORMATION

Corresponding Author

*E-mail: csonkagi@gmail.com

Notes

The authors declare no competing financial interest.

■ ACKNOWLEDGMENTS

The authors acknowledge helpful discussions with J.P. Perdew. B.X. thanks to Dr. Feng Jing the results of the phonon calculations. This work was supported in part by the National Science Foundation under grant no. DMR-0854769 and under cooperative agreement no. EPS-1003897 with additional support from the Louisiana Board of Regents. Part of the research was done with high-performance computational resources provided by the Louisiana Optical Network Initiative.

■ REFERENCES

(1) Perdew, J. P.; Schmidt, K. In Density Functional Theory and Its Applications to Materials, 1st ed.; van Doren, V. E., van Alsenoy, C., Ernzerhof, M., Eds; Springer: New York, 2001.

(2) Perdew, J. P.; Burke, K.; Ernzerhof, M. *Phys. Rev. Lett.* **1996**, *77*, 3865−3868.

(3) Csonka, G. I.; Vydrov, O. A.; Scuseria, G. E.; Ruzsinszky, A.; Perdew, J. P. *J. Chem. Phys.* **2007**, *126*, 244107.

(4) Tao, J.; Perdew, J. P.; Staroverov, V. N.; Scuseria, G. E. *Phys. Rev. Lett.* **2003**, *91*, 146401.

(5) Perdew, J. P.; Ruzsinszky, A.; Csonka, G.; Vydrov, O. A.; Scuseria, G. E.; Constantin, L. A.; Zhou, X.; Burke, K. *Phys. Rev. Lett.* **2008**, *100*, 136406.

(6) Perdew, J.; Ruzsinszky, A.; Csonka, G.; Constantin, L.; Sun, J. *Phys. Rev. Lett.* **2009**, *103*, 026403(E); **2011**, *106*, 179902.

(7) Lee, D.; Constantin, L. A.; Perdew, J. P.; Burke, K. *J. Chem. Phys.* **2009**, *130*, 034107.

(8) Ma, S.-K.; Brueckner, K. *Phys. Rev.* **1968**, *165*, 18−31.

(9) Hu, C.; Langreth, D. *Phys. Rev. B* **1986**, *33*, 943−959.

(10) Svendsen, P.; von Barth, U. *Phys. Rev. B* **1996**, *54*, 17402−17413.

(11) Perdew, J. P.; Tao, J.; Staroverov, V. N.; Scuseria, G. E. *J. Chem. Phys.* **2004**, *120*, 6898−911.

(12) Sun, J.; Xiao, B.; Ruzsinszky, A. http://arxiv.org/abs/1203.2308.

(13) Kresse, G.; Joubert, D. *Phys. Rev. B* **1999**, *59*, 1758−1775.

(14) Frisch, M. J.; Trucks, G. W.; Schlegel, H. B.; Scuseria, G. E.; Robb, M. A.; Cheeseman, J. R.; Montgomery, J. A., Jr.; Vreven, T.; Kudin, K. N.; Burant, J. C.; Millam, J. M.; Iyengar, S. S.; Tomasi, J.; Barone, V.; Mennucci, B.; Cossi, M.; Scalmani, G.; Rega, N.; Petersson, G. A.; Nakatsuji, H.; Hada, M.; Ehara, M.; Toyota, K.; Fukuda, R.; Hasegawa, J.; Ishida, M.; Nakajima, T.; Honda, Y.; Kitao, O.; Nakai, H.; Klene, M.; Li, X.; Knox, J. E.; Hratchian, H. P.; Cross, J. B.; Bakken, V.; Adamo, C.; Jaramillo, J.; Gomperts, R.; Stratmann, R. E.; Yazyev, O.; Austin, A. J.; Cammi, R.; Pomelli, C.; Ochterski, J. W.; Ayala, P. Y.; Morokuma, K.; Voth, G. A.; Salvador, P.; Dannenberg, J. J.; Zakrzewski, V. G.; Dapprich, S.; Daniels, A. D.; Strain, M. C.; Farkas, O.; Malick, D. K.; Rabuck, A. D.; Raghavachari, K.; Foresman, J. B.; Ortiz, J. V.; Cui, Q.; Baboul, A. G.; Clifford, S.; Cioslowski, J.; Stefanov, B. B.; Liu, G.; Liashenko, A.; Piskorz, P.; Komaromi, I.; Martin, R. L.; Fox, D. J.; Keith, T.; Al-Laham, M. A.; Peng, C. Y.; Nanayakkara, A.; Challacombe, M.; Gill, P. M. W.; Johnson, B.; Chen, W.; Wong, M. W.; Gonzalez, C.; Pople, J. A. *Gaussian 03*, revision B.05; Gaussian, Inc.: Pittsburgh, PA, 2005.

(15) Csonka, G. I.; Perdew, J. P.; Ruzsinszky, A. *J. Chem. Theory Comput.* **2010**, *6* (12), 3688−3703.
(16) Lynch, B. J.; Truhlar, D. G. *J. Phys. Chem. A* **2003**, *107*, 8996−8999; **2004**, *108*, 1460(E).
(17) Csonka, G. I.; Ruzsinszky, A.; Tao, J. M.; Perdew, J. P. *Int. J. Quantum Chem.* **2005**, *101*, 506−511.
(18) Curtiss, L. A.; Raghavachari, K.; Redfern, P. C.; Pople, J. A. *J. Chem. Phys.* **2000**, *112*, 7374−7383.
(19) Csonka, G. I.; Perdew, J. P.; Ruzsinszky, A.; Philipsen, P. H. T.; Lebègue, S.; Paier, J.; Vydrov, O.; Ángyán, J. G. *Phys. Rev. B* **2009**, *79*, 155107.
(20) Hao, P.; Fang, Y.; Sun, J.; Csonka, G. I.; Philipsen, P. H. T.; Perdew, J. P. *Phys. Rev. B* **2012**, *85*, 014111.
(21) Schimka, L.; Harl, J.; Kresse, G. *J. Chem. Phys.* **2011**, *134*, 024116.
(22) Kittel, C. *Introduction to Solid State Physics*; Wiley: New York, 1996.
(23) Alchagirov, A.; Perdew, J.; Boettger, J.; Albers, R.; Fiolhais, C. *Phys. Rev. B* **2001**, *63*, 224115.
(24) Monkhorst, H. J.; Pack, J. D. *Phys. Rev. B* **1976**, *13*, 5188−5192.
(25) Mujica, A.; Rubio, A.; Muñoz, A.; Needs, R. *Rev. Mod. Phys.* **2003**, *75*, 863−912.
(26) Hennig, R. G.; Wadehra, A.; Driver, K. P.; Parker, W. D.; Umrigar, C. J.; Wilkins, J. W. *Phys. Rev. B* **2010**, *82*, 014101.
(27) Batista, E. R.; Heyd, J.; Hennig, R. G.; Uberuaga, B. P.; Martin, R. L.; Scuseria, G. E.; Umrigar, C. J.; Wilkins, J. W. *Phys. Rev. B* **2006**, *74*, 121102 (R).
(28) McMahon, M. I.; Nelmes, R. J.; Wright, N. G.; Allan, D. R. *Phys. Rev. B* **1994**, *50*, 739−743.
(29) Maezono, R.; Drummond, N. D.; Ma, A.; Needs, R. J. *Phys. Rev. B* **2010**, *82*, 184108.
(30) Holm, J. L.; Kleppa, O. J., Jr.; Westrum, E. F. *Geochim. Cosmochim. Acta* **1967**, *31*, 2289−2307.
(31) Akaogi, M.; Navrotsky, A. *Phys. Earth Planet. Inter.* **1984**, *36*, 124−134.
(32) Driver, K. P.; Cohen, R. E.; Wu, Z.; Militzer, B.; López Ríos, P.; Towler, M. D.; Needs, R. J.; Wilkins, J. W. *Proc. Natl. Acad. Sci. U.S.A.* **2010**, *107*, 9519−9524.
(33) Clark, S. J.; Segall, M. D.; Pickard, C. J.; Hasnip, P. J.; Probert, M. I. J.; Refson, K.; Payne, M. C. *Z. Kristallogr.* **2005**, *220*, 567−570.
(34) Csonka, G. I.; Erdősy, M.; Réffy, J. *J. Comput. Chem.* **1994**, *15*, 925−936.
(35) Csonka, G. I.; Réffy, J. *Chem. Phys. Lett.* **1994**, *229*, 191−197.
(36) Carteret, C.; Labrosse, A.; Assfeld, X. *Spectrochim. Acta, Part A* **2007**, *67*, 1421−9.
(37) Al Derzi, A. R.; Gregušová, A.; Runge, K.; Bartlett, R. J. *Int. J. Quantum Chem.* **2008**, *108*, 2088−2096.
(38) Abild-Pedersen, F.; Andersson, M. P. *Surf. Sci.* **2007**, *601*, 1747−1753.
(39) Feibelman, P. J.; Hammer, B.; Norskov, J. K.; Wagner, F.; Scheffler, M.; Stumpf, R.; Watwe, R.; Dumesic, J. *J. Phys. Chem. B* **2001**, *105*, 4018−4025.
(40) Schimka, L.; Harl, J.; Stroppa, A.; Grueneis, A.; Marsman, M.; Mittendorfer, F.; Kresse, G. *Nat. Mater.* **2010**, *9*, 741−744.
(41) Sun, J.; Marsman, M.; Ruzsinszky, A.; Kresse, G.; Perdew, J. P. *Phys. Rev. B* **2011**, *83*, 121410(R).